UNIVERSITY *of* York

This is a repository copy of *Life in a Random Universe: Sciama's Argument Reconsidered*.

White Rose Research Online URL for this paper:
https://eprints.whiterose.ac.uk/id/eprint/209141/

Version: Published Version

Article:

CrossMark

Life in a Random Universe: Sciama's Argument Reconsidered

Zhi-Wei Wang[1,2] and Samuel L. Braunstein[3]

[1] College of Physics, Jilin University, Changchun 130012, People's Republic of China; zhiweiwang.phy@gmail.com
[2] Department of Physics, University of Warwick, Coventry CV4 7AL, UK
[3] Computer Science, University of York, York YO10 5GH, UK; sam.braunstein@york.ac.uk

Abstract

Random sampling in high dimensions has successfully been applied to phenomena as diverse as nuclear resonances, neural networks, and black hole evaporation. Here we revisit an elegant argument by the British physicist Dennis Sciama, who demonstrated that were our Universe random, it would almost certainly have a negligible chance for life. Under plausible assumptions, we show that a random universe can masquerade as "intelligently designed," with the fundamental constants instead appearing to be fined tuned to achieve the highest probability for life to occur. For our Universe, this mechanism may only require there to be around a dozen currently unknown fundamental constants. We speculate on broader applications for the mechanism we uncover.

Unified Astronomy Thesaurus concepts: Anthropic principle (48); Cosmology (343); Astrobiology (74); Search for extraterrestrial intelligence (2127)

1. Introduction

Whatever might be eventually concluded about a universal definition for life, we can certainly agree that the Universe we inhabit has so far supported the emergence, evolution, and continued sustenance of human beings. Despite our having grown collectively more powerful than most known species, within the Universe we are very fragile and maintain a precarious hold on existence. We are carbon based, requiring a planetary body to live on, which follows a comfortable and steady orbit around a single and not too energetic star.

These constraints already place tight bounds on the fundamental constants of the Universe. To ensure that a population of yellow dwarf stars like our Sun exist, the fine structure constant must be tuned to within a percent or two of its current value (outside this narrow range almost all stars would either be blue giants or red dwarfs; Thorne et al. 2000). The cosmological constant must be between 120 and 124 orders of magnitude smaller than its naive quantum field theoretic value. The upper bound ensures that bodies can form gravitationally (Weinberg 1987; Martel et al. 1998) and the lower bound ensures that nascent life will not be extinguished by the proximity to gamma-ray bursts (Piran et al. 2016). To ensure that nuclear reactions within stars can form carbon, but not have the process bypassed leaving only oxygen, a remarkable set of coincidences is required among the fundamental constants so that one resonant energy level exists, yet another level just fails to be resonant (Hoyle 1954). Many of the fundamental constants therefore seem to be boxed into a narrow range of values compatible with our existence (Carter 1974). Of course, a less anthropocentric view would considerably broaden this range (Adams 2019; see Section 4).

How can we understand our being in such a human-compatible Universe? It has been suggested (Dicke 1961) that the fundamental constants may have been selected "randomly" among all possible values. If that were the case, then such

compatibility is merely a condition consistent with our being here to observe it. Given enough potential universes to randomly choose from almost anything *could* happen, and the conditional probability for human compatibility would be one. Equivalently, if these "random selections" were individual universes within a multiverse, then our Universe being human compatible would be the same as us being located in one of the universes within the multiverse where humans are possible. In other words, given enough potential universes almost anything *will* happen. Such "explanations" are said to invoke the weak anthropic principle (Carter 1974), yet they explain nothing and fail to provide any real resolution. Are they at least predictive?

Dennis Sciama, considered to be one of the fathers of modern cosmology, argued that were our Universe random, in either sense given above, then it would almost certainly have a low probability for life as we know it (Deutsch 2011; Wang & Braunstein 2023).

Sciama assumed that the feature distinguishing different potential universes was the set of specific values taken by the fundamental constants; the underlying physical laws themselves being fixed. We can then envision the human-compatible universes as an "island" within a "sea" of more general possibilities. Each point on the island or in the sea describes a unique universe that is described by a distinct set of fundamental constants. The dimensionality of this space of points is naively given by the number of fundamental constants. Thus the human-compatible island of universes corresponds to some shape in a space. The shoreline of the island corresponds to the boundary separating universes with a chance for human life to form from those where this is impossible. Thus, the shoreline itself will be made up of universes with an exactly vanishing probability for such life. Assuming continuity, as one moves inland, this probability will increase, reaching a maximum presumably somewhere far in from the shoreline.

This probability landscape is different from the chance of randomly selecting a universe. Because the range of parameters consistent with human life is quite small, one might expect any smooth measure for randomly selecting universes to be approximately uniform across the island. Sciama's argument
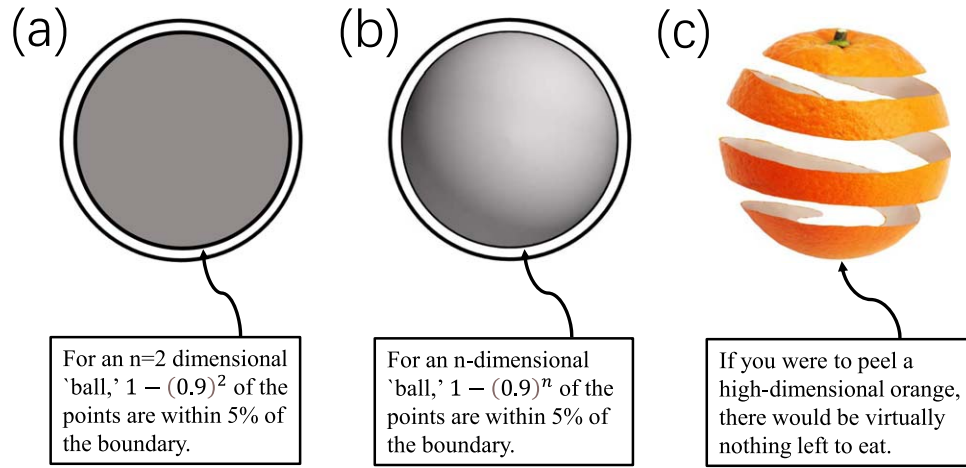
Figure 1. An "unappealing" consequence of concentration-of-measure phenomena: (a) an n = two-dimensional "ball" has a $1 - (0.9)^2 = 0.19$ fraction of points within 5% of the boundary; (b) an n = three-dimensional ball has fraction $1 - (0.9)^3 = 0.271$ within 5% of the boundary; for large n, the fraction $1 - (0.9)^n$ approaches unity. Therefore, (c) if you were to peel a high-dimensional orange, there would be almost nothing left behind!

now follows from a well-known concentration-of-measure phenomenon (Milman 1988), described as follows.

Consider an n-dimensional cube (a hypercube) with side length s and hence volume $s \times s \times \cdots \times s = s^n$. Now suppose you paint this hypercube, causing the side length to marginally increase to $s + \delta$. The volume of the paint used is simply $(s + \delta)^n - s^n \geqslant n \, s^{n-1} \delta$. But even if the layer of paint is very thin, so $\delta \ll s$, in sufficiently high dimensions, $n \geqslant s/\delta$, the volume of the paint will exceed the volume of the original hypercube. Thus, were we to grind up our thinly painted hypercube and take a random sample, we would most likely find paint!

This is not only true for hypercubes, but for any shape in high dimensions (Milman 1988). The volume, and similarly the weight, will be entirely concentrated within a thin layer at the surface. Thus, figuratively, a high-dimensional orange is essentially only its peel. See Figure 1.

Applied to the high-dimensional island of human-compatible universes, a randomly selected universe will then almost certainly be found in a narrow band on the shore. However, since there is no chance for life at the shoreline or anywhere off the island, the probability for life would be expected to be very low for a typical random universe lying in this narrow band at the shore.

This prediction is in contrast to that of intelligent design where one might expect a universe further inland closer to, or possibly achieving, the greatest chance for human life.

2. Method

Is this space of universes really high dimensional? In 1936 Eddington counted four fundamental constants (Eddington 1936). This count excludes Newton's gravitational constant, the speed of light, Planck's constant, and the permittivity of the vacuum, all used to provide scales for dimensional quantities like length, time, mass and electric charge (Eddington 1936). Just a few years ago this count had grown to 26 for the "standard model," including the cosmological constant for gravity (Siegel 2018). Today, if we add three neutrino masses, the count would be 29. However, our current model of the Universe hardly explains everything. There remain numerous long-standing open questions, many cosmological in nature, such as matter–antimatter asymmetry,

dark matter, dark energy, and more. Thus it would be surprising if the total number of fundamental constants in a complete theory of the Universe were not much larger.

Although it did not figure into Sciama's original argument, we shall see that the shape of the island plays a crucial role in the possible apparent reversal of Sciama's conclusion. Note that the "orange peel" result itself is essentially independent of this shape, which follows simply from the scaling of the "hypervolume" with dimensionality. Thus, there is no question about a randomly selected universe compatible with human life having a set of fundamental constants that almost certainly lie on the narrow shore, with a low chance for life like us.

Notwithstanding this, where on the island the Universe appears to lie can depend on the island's shape. This can be the case whenever our knowledge of the list of fundamental constants is incomplete. In this case, we would consider the island and its surrounding sea to be a lower-dimensional space than it actually is. Our view of the island would be one that projects out the unknown constants. This may be visualized as an "X-ray" of the actual n-dimensional island onto a lower m-dimensional island describing the known constants. See Figure 2.

3. Results

In the case that the island has the shape of a uniform-weight n-dimensional cube (a hypercube), with independent bounds on each constant, the X-ray is simply a lower-dimensional uniform-weight hypercube. See Figure 2(a). Again the lower-dimensional shore contains the greatest weight.

By contrast, for a uniform-weight hyperball-shaped island, the X-ray, integrating out many dimensions, leads to a narrow Gaussian with the weight concentrated at the center of the island, far inland from the shoreline (see the Appendix A). See Figure 2(b). Further, if the uniform-weight n-dimensional hypercube is X-rayed along a skewed orientation (e.g., one randomly chosen) the projected island is again well approximated by a Gaussian with the weight concentrated at the center of the island (see the Appendix C). See Figure 2(c).

Surprisingly, the result we find for a hyperball-shaped island shown in Figure 2(b), or equivalently, the skew-oriented hypercube-shaped island shown in Figure 2(c), may well represent the generic result.
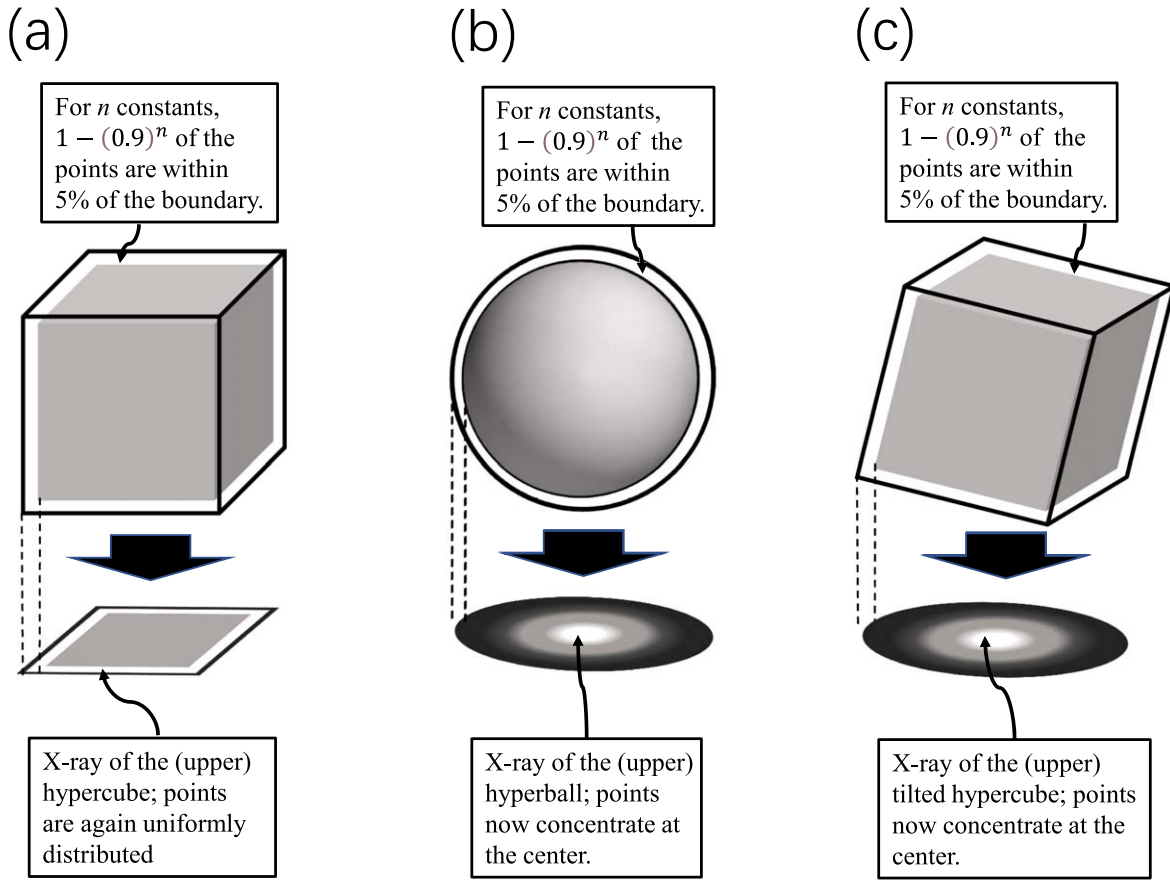
(a)

For n constants, $1 - (0.9)^n$ of the points are within 5% of the boundary.

X-ray of the (upper) hypercube; points are again uniformly distributed

(b)

For n constants, $1 - (0.9)^n$ of the points are within 5% of the boundary.

X-ray of the (upper) hyperball; points now concentrate at the center.

(c)

For n constants, $1 - (0.9)^n$ of the points are within 5% of the boundary.

X-ray of the (upper) tilted hypercube; points now concentrate at the center.

Figure 2. Random sampling from the human-compatible island can look different dependent on its shape, if one has only limited access to the fundamental constants. The high-weight region (typically the "shore") is shown in white, with the remaining low-weight contribution in gray. The island of the accessible fundamental constants is obtained by integrating out those constants which are unknown or unobserved; this is visualized as an "X-ray" of the actual island. (a) For an island which is an n-dimensional hypercube (upper), an X-ray reduces to a uniform-measure hypercube in a lower dimension (lower). (b) For an island which is a uniformly distributed n-dimensional ball (upper) with many unknown constants, its X-ray is well approximated by a narrow Gaussian concentrated at the center of the human-compatible island (lower). (c) For an island which is an n-dimensional hypercube (upper), an X-ray along a randomly oriented direction is again well approximated by a Gaussian concentrated at the center of the human-compatible island (lower).

First, the human-compatible island will be formed by those universes whose fundamental constants simultaneously satisfy a series of human-compatible constraints. Each of these constraints may be thought of as dividing the space of all possible universes into two subsets: those that satisfy a specific constraint for life and those that fail to. Now, as already mentioned, the range of parameters consistent with human life is quite small; the island itself is in some sense "small." Consequently, assuming each constraint is smooth, its action constraining our island should be well approximated locally by a separating hyperplane in the space of universes. Combining the hyperplanes of these individual human-compatible constraints then yields a description of the human-compatible universes as well approximated by a convex-faceted island.

Second, the various correlations and coincidences found among the fundamental constants when determining the human-compatible island's shoreline (Eddington 1939; Hoyle 1954; Carter 1974) suggest that the facets associated with such correlations will be tilted with respect to the axes given by the fundamental constants themselves. Combined, these arguments yield a convex island whose facets have a skewed orientation.

Finally, the projective central limit theorem (Diaconis & Freedman 1984; Klartag 2007) ensures that virtually any projection of such a high n-dimensional uniform-weight shape will be well approximated by a Gaussian with variance scaling as $1/n$ (with respect to a suitably chosen diameter).

However, the projective central limit theorem only tells us that the distribution is peaked far inland from the accessible (projected) shoreline as $n \to \infty$ (for the hyperball, in fact we find that $m/n \ll 1$ is sufficient; see the Appendix A). What about the probability for the accessible parameters nevertheless being found on the projected shore near the boundary? We find a universal behavior for the tail of the distribution of the projected hyperball as $m/n \to 1$. In particular, in Figure 3 we compute the probability to be within 5% of the projected shoreline versus the fraction of accessible constants, m/n, when an n-dimensional hyperball is projected down to m dimensions. For $n \in \{42, 100, 250\}$, we see that if less than a threshold of around 80% of the total number of fundamental constants are accessible, then the chance of being near the boundary is less than around 0.35. Thus, taking as the null hypothesis that our Universe is random, there would be a low chance for finding the fundamental constants of the Universe to be near the shoreline until we had knowledge of the vast majority of all the Universe's parameters.

4. Discussion and Summary

In summary, Sciama's reasoning suggests that were our Universe random, there would be a statistical signature

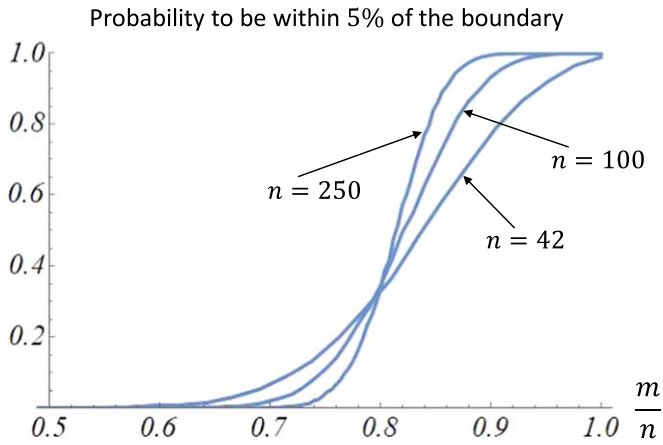## Probability to be within 5% of the boundary

Figure 3. Probability for the m accessible constants of a random universe to be within 5% of the life-denying boundary vs. the accessible fraction m/n. The calculation assumes the island has the shape of a hyperball with n fundamental constants, though the existence of only m is known. We consider $n \in \{42, 100, 250\}$. In each case, unless at least 80% of the total number of constants are accessible ($m/n \geqslant 0.8$), the chance of being near the boundary is less than $\simeq 0.35$.

whereby the fundamental constants would almost certainly lie near the boundary of human-compatible universes.

One might view Sciama's result to be solely that a random universe would lead to a scenario where life as we know it is only barely possible. This "orange peel" argument stands firm and may even explain the apparent scarcity of intelligent life in the Universe, potentially resolving Fermi's paradox (Deutsch 2011; Ćirković 2016). However, since the island of parameters consistent with any type of life-form would appear to be significantly larger (Adams 2019) than that considered solely for the sake of humans, it is likely that life itself may be very common in our Universe. This rough-and-ready prediction for a random universe may well be falsifiable within the coming years.

However, presuming that our knowledge of the fundamental constants is incomplete, we have shown the signature for a random universe can be reversed. For example, were our Universe random with 42 fundamental constants (instead of the merely 29 currently known), and taking the shape of the human-compatible island of parameters as discussed above, there would be only $\simeq 5.5\%$ chance of the set of those 29 currently known constants to lie within 5% of the boundary where human life becomes impossible. Instead, the greatest likelihood would be to find these known constants to be far within the "projected" human-compatible island of universes, mimicking a universe built by intelligent design to create intelligence.

Currently there is no direct evidence to support the claim that Sciama's statistical signature applies to our Universe (outside of consistency with the null results from SETI; Overbye 2020). However, this observation is in the context of fundamental theories which cannot yet explain everything about our Universe, so there is a widely accepted expectation that new physics, along with additional fundamental constants, would be needed. Further, our current best guess for a fundamental theory, string theory, naturally contains a multiverse and hence a random selection mechanism. Combined with our analysis above, these reasoned expectations suggest the statistical prediction that *at least* around a dozen fundamental constants,

and possibly many more, are yet to be discovered to explain our Universe fully.

Can any wider scientific lesson be learned from our arguments? Beyond the anthropic issues discussed here, they may be relevant to astronomy and indeed any field when viewed as a data science. After all, our analysis suggests potential pitfalls when considering how to interpret data sampled from constrained sets. In particular, unknown degrees of freedom are common in some systems and the viewing of low-dimensional "sections" of high-dimensional data is virtually the sine qua non of any data science strategy.

Finally, humanity's looking out to the stars has always had at its heart a search for meaning. Curiously, it may well be that our analysis here shows, *not* how to create meaning 'out of whole cloth,' but how to enhance any scintilla greatly.

Indeed, if we consider the intelligent design of the Universe as an artful act, whatever else it might be, then we have uncovered a mechanism whereby even a random universe may appear artful; or loosely speaking, whereby even an atheist might say (Wilde 1889) "life imitates art." Recalling that our analysis is based on concentration-of-measure phenomena in high-dimensional spaces, it is natural to ask whether this mechanism for imitating art may not have grander application. For example, could one enhance the artfulness of an almost soullessly generated piece of "art" to make it mimic a true work of art; not by slavish copying, but perhaps by so constraining the work around with interconnections and correlations—the coincidences constraining our fundamental constants—that one may begin to find it harder to distinguish between such a piece and an intelligently crafted work? These correlations acting to "tilt the facets of our island" and so produce an apparent lower-dimensional artful enhancement. For something complex, having a sufficient number of working parts, it may not even be necessary to hide part of the work; or as with our analysis here, it may be crucial to first build the work and then make large portions inaccessible—be they backstory, foundation, milieu, history, whatever. And if anything like this can succeed, why not look further, perhaps toward the imitation of intelligence itself. Maybe the magic behind creating meaning has "simply" been a matter of hiding much of the supporting artifice from the audience, and even from ourselves.

Appendix A
Projection of an $(n-1)$ Sphere to One Dimension

Consider a smooth convex n-dimensional geometric body with a uniform probability distribution across and within it. The projective central limit theorem claims that as $n \to \infty$, if we project such a body to lower dimensions, the probability will concentrate to a "center" of the lower-dimensional object (Diaconis & Freedman 1984; Klartag 2007; Knaeble 2015). This phenomenon has been proved for all smooth convex geometric bodies and the limiting probability distribution is claimed to be a Gaussian distribution with variance scaling as $1/n$.

Here we compute this exactly for an $(n-1)$ sphere (the surface of an n-dimensional ball) projected to m dimensions. We find for large $n-m$ that the resulting distribution is Gaussian

with variance scaling as $1/n$. This is in agreement with the more general, though looser, claim of the projective central limit theorem when $n \gg m$. Finally, combining the "orange peel" concentration-of-measure result, we argue that the same limit to a Gaussian with variance scaling as $1/n$ will hold for the projection of an n-dimensional ball onto m dimensions.

Because the general calculation is rather complicated, we start with the simpler case of projecting an $(n-1)$ sphere onto a single dimension.

An $(n-1)$ sphere with unit radius in n-dimensional Euclidean space (Cartesian coordinates) may be described as satisfying $x_1^2 + x_2^2 + \cdots + x_n^2 = 1$. It may be transformed into hyperspherical coordinates by

$$
\begin{aligned}
x_1 &= -\cos \varphi_1 \\
x_2 &= -\sin \varphi_1 \cos \varphi_2 \\
&\vdots \\
x_{n-1} &= -\sin \varphi_1 \sin \varphi_2 \cdots \cos \varphi_{n-1} \\
x_n &= -\sin \varphi_1 \sin \varphi_2 \cdots \sin \varphi_{n-1},
\end{aligned}
\tag{A1}
$$

where $\varphi_1, \varphi_2, \ldots, \varphi_{n-2} \in [0, \pi]$ and $\varphi_{n-1} \in [0, 2\pi]$. Here the minus sign is just for future convenience; note that each x_i is not sensitive to such a minus sign.

Then in hyperspherical coordinates, the volume element of such an $(n-1)$ sphere may be written as

$$
\begin{aligned}
d\Omega_{n-1} = \sin^{n-2}(\varphi_1) \sin^{n-3}(\varphi_2) \cdots \sin^2(\varphi_{n-3}) \\
\times \sin(\varphi_{n-2}) \, d\varphi_1 d\varphi_2 \cdots d\varphi_{n-2} d\varphi_{n-1},
\end{aligned}
\tag{A2}
$$

as is easily checked by computing the Jacobian for this transformation. Integrating this volume element over the entire sphere yields the standard result

$$
\begin{aligned}
S_{n-1} &= \int d\Omega_{n-1} \\
&= \int \sin^{n-2}(\varphi_1) \sin^{n-3}(\varphi_2) \\
&\quad \cdots \sin^2(\varphi_{n-3}) \sin(\varphi_{n-2}) \, d\varphi_1 d\varphi_2 \cdots d\varphi_{n-2} d\varphi_{n-1} \\
&= \pi^{\frac{n-2}{2}} \frac{\Gamma\left(\frac{n-1}{2}\right)}{\Gamma\left(\frac{n}{2}\right)} \frac{\Gamma\left(\frac{n-2}{2}\right)}{\Gamma\left(\frac{n-1}{2}\right)} \cdots \frac{\Gamma\left(\frac{2}{2}\right)}{\Gamma\left(\frac{3}{2}\right)} 2\pi \\
&= \frac{2\pi^{\frac{n}{2}}}{\Gamma\left(\frac{n}{2}\right)},
\end{aligned}
\tag{A3}
$$

where $\Gamma(n)$ is the gamma function, so $\Gamma(1) = 1$, and in moving from the second to the third line we have used the result that

$$
\int_0^\pi \sin^m(\varphi) d\varphi = \sqrt{\pi} \, \frac{\Gamma\left(\frac{m+1}{2}\right)}{\Gamma\left(\frac{m+2}{2}\right)}.
\tag{A4}
$$

We now consider projecting the uniformly distributed $(n-1)$ sphere onto a single dimension (i.e., the case $m=1$). Normalizing the measure of Equation (A2) by S_{n-1}, we may

compute the expectation of a general function of φ_1 as

$$
\begin{aligned}
\langle f(\varphi_1) \rangle &= \frac{1}{S_{n-1}} \int f(\varphi_1) d\Omega_{n-1} \\
&= \frac{1}{S_{n-1}} \int_0^\pi f(\varphi_1) \sin^{n-2}(\varphi_1) \, \pi^{\frac{n-3}{2}} \frac{\Gamma\left(\frac{n-2}{2}\right)}{\Gamma\left(\frac{n-1}{2}\right)} \frac{\Gamma\left(\frac{n-3}{2}\right)}{\Gamma\left(\frac{n-2}{2}\right)} \\
&\quad \cdots \frac{\Gamma\left(\frac{2}{2}\right)}{\Gamma\left(\frac{3}{2}\right)} 2\pi \, d\varphi_1 \\
&= \frac{\Gamma\left(\frac{n}{2}\right)}{2\pi^{\frac{n}{2}}} \int_0^\pi f(\varphi_1) \sin^{n-2}(\varphi_1) \frac{2\pi^{\frac{n-1}{2}}}{\Gamma\left(\frac{n-1}{2}\right)} d\varphi_1 \\
&= \int_0^\pi f(\varphi_1) \sin^{n-2}(\varphi_1) \frac{\Gamma\left(\frac{n}{2}\right)}{\sqrt{\pi} \, \Gamma\left(\frac{n-1}{2}\right)} d\varphi_1.
\end{aligned}
\tag{A5}
$$

Consequently, the distribution of φ_1 is given by

$$
P(\varphi_1) d\varphi_1 = \sin^{n-2}(\varphi_1) \frac{\Gamma\left(\frac{n}{2}\right)}{\sqrt{\pi} \, \Gamma\left(\frac{n-1}{2}\right)} d\varphi_1, \qquad \varphi_1 \in [0, \pi].
\tag{A6}
$$

To see the probability distribution in Euclidean space, we need to transform Equation (A6) back to the coordinate x_1. Since $x_1 = -\cos \varphi_1$, we have $dx_1 = \sin \varphi_1 d\varphi_1$ and $\sin(\varphi_1) = \sqrt{1 - x_1^2}$, and hence we obtain

$$
P(x_1) dx_1 = \frac{\Gamma\left(\frac{n}{2}\right)}{\sqrt{\pi} \, \Gamma\left(\frac{n-1}{2}\right)} (1 - x_1^2)^{\frac{n-3}{2}} dx_1, \qquad x_1 \in [-1, 1].
\tag{A7}
$$

We may also obtain an exact expression for the variance

$$
(\Delta x_1)^2 = \frac{1}{n}.
\tag{A8}
$$

It is easy to see that this probability distribution gets narrower and narrower as n increases. Using the result that $\lim_{n \to \infty} \left(1 - \frac{x}{n}\right)^n = e^{-x}$ we see that for sufficiently small x_1 and large n Equation (A7) may be approximated by a Gaussian with variance $1/n$, for the case $m = 1$. This result is in exact agreement with that given in previous work (Knaeble 2015), and we shall see below that the exact result yields a subtly different outcome for $m > 1$.

Appendix B
Projecting to m Dimensions

When projecting an $(n-1)$ sphere onto m Cartesian dimensions, the logic is similar to that given in the previous section but now we will need to integrate out the angles from

the set $\{\varphi_{m+1}, \varphi_{m+2},...,\varphi_{n-1}\}$. Thus, we find

$$
\langle f(\varphi_1,...,\varphi_m) \rangle = \frac{1}{S_{n-1}} \int f(\varphi_1,...,\varphi_m) d\Omega_{n-1}
$$

$$
= \frac{1}{S_{n-1}} \int_0^\pi \cdots \int_0^\pi f(\varphi_1,...,\varphi_m) \sin^{n-2}(\varphi_1) \sin^{n-3}(\varphi_2) \cdots \sin^{n-m-1}(\varphi_m)
$$

$$
\times \pi^{\frac{n-m-2}{2}} \frac{\Gamma(\frac{n-m-1}{2})}{\Gamma(\frac{n-m}{2})} \frac{\Gamma(\frac{n-m-2}{2})}{\Gamma(\frac{n-m-1}{2})} \cdots \frac{\Gamma(\frac{2}{2})}{\Gamma(\frac{3}{2})} 2\pi \, d\varphi_1 d\varphi_2 \cdots d\varphi_m
$$

$$
= \frac{\Gamma(\frac{n}{2})}{2\pi^{\frac{n}{2}}} \int_0^\pi \cdots \int_0^\pi f(\varphi_1,...,\varphi_m) \sin^{n-2}(\varphi_1) \sin^{n-3}(\varphi_2) \cdots \sin^{n-m-1}(\varphi_m) \frac{2\pi^{\frac{n-m}{2}}}{\Gamma(\frac{n-m}{2})} d\varphi_1 d\varphi_2 \cdots d\varphi_m
$$

$$
= \int_0^\pi \cdots \int_0^\pi f(\varphi_1,...,\varphi_m) \sin^{n-2}(\varphi_1) \sin^{n-3}(\varphi_2) \cdots \sin^{n-m-1}(\varphi_m) \frac{\Gamma(\frac{n}{2})}{\pi^{\frac{m}{2}}\Gamma(\frac{n-m}{2})} d\varphi_1 d\varphi_2 \cdots d\varphi_m. \tag{B1}
$$

Since the volume element described by two different coordinates systems may be connected by the Jacobian, we have

$$
dx_1 dx_2 \cdots dx_m = J \, d\varphi_1 d\varphi_2 \cdots d\varphi_m, \tag{B2}
$$

where J is the Jacobian describes this volume transformation. From Equation (A1), we know that J may be written as

$$
J = \left| \frac{\partial x_i}{\partial \varphi_j} \right| = \begin{vmatrix} \sin\varphi_1 & 0 & \cdots & 0, \\ \cos\varphi_1 \cos\varphi_2 & \sin\varphi_1 \sin\varphi_2 & \cdots & 0, \\ \vdots & \vdots & \ddots & \vdots, \\ \cos\varphi_1 \sin\varphi_2 \cdots \sin\varphi_{m-1}\cos\varphi_m & \sin\varphi_1 \cos\varphi_2 \cdots \sin\varphi_{m-1}\cos\varphi_m & \cdots & \sin\varphi_1 \cdots \sin\varphi_m. \end{vmatrix} \tag{B3}
$$

Since terms in the upper triangle in the Jacobian, Equation (B3), are all zero, the Jacobian trivially reduces to

$$
J = \sin^m(\varphi_1) \sin^{m-1}(\varphi_2) \cdots \sin(\varphi_m). \tag{B4}
$$

Inserting Equation (B4) into Equation (B2) yields

$$
dx_1 dx_2 \cdots dx_m = \sin^m(\varphi_1) \sin^{m-1}(\varphi_2) \cdots \sin(\varphi_m) \, d\varphi_1 d\varphi_2 \cdots d\varphi_m, \tag{B5}
$$

and substituting Equation (B5) into Equation (B1) yields

$$
\langle f(\varphi_1,...,\varphi_m) \rangle
$$

$$
= \int_{-1}^1 \int_{-\sin\varphi_1}^{\sin\varphi_1} \cdots \int_{-\sin(\varphi_1)\cdots\sin(\varphi_{m-1})}^{\sin(\varphi_1)\cdots\sin(\varphi_{m-1})} f(\varphi_1,...,\varphi_m) \sin^{n-m-2}(\varphi_1) \sin^{n-m-2}(\varphi_2) \cdots \sin^{n-m-2}(\varphi_m)
$$

$$
\times \frac{\Gamma\left(\frac{n}{2}\right)}{\pi^{\frac{m}{2}}\Gamma\left(\frac{n-m}{2}\right)} dx_1 dx_2 \cdots dx_m, \tag{B6}
$$

where $\sin(\varphi_i)$ is positive function of x_i.

To simplify Equation (B6) further, let us first consider $x_1^2 + x_2^2 + \cdots + x_m^2$. From Equation (A1), this may be written as

$$
x_1^2 + x_2^2 + \cdots + x_m^2 = \cos^2(\varphi_1) + \sin^2(\varphi_1)\cos^2(\varphi_2) + \cdots + \sin^2(\varphi_1)\sin^2(\varphi_2) \cdots \cos^2(\varphi_m)
$$

$$
= \cos^2(\varphi_1) + \sin^2(\varphi_1)(1 - \sin^2(\varphi_2)) + \cdots + \sin^2(\varphi_1)\sin^2(\varphi_2) \cdots \cos^2(\varphi_m)
$$

$$
= 1 - \sin^2(\varphi_1)\sin^2(\varphi_2) + \cdots + \sin^2(\varphi_1)\sin^2(\varphi_2) \cdots \cos^2(\varphi_m). \tag{B7}
$$

The above procedure can be repeated until we arrive at

$$
x_1^2 + x_2^2 + \cdots + x_m^2 = 1 - \sin^2(\varphi_1)\sin^2(\varphi_2) \cdots \sin^2(\varphi_m). \tag{B8}
$$

Applying Equation (B8) to Equation (B6) then gives

$$\langle f(x_1,\ldots,x_m)\rangle$$

$$= \int_{-1}^{1} \int_{-\sqrt{1-x_1^2}}^{\sqrt{1-x_1^2}} \cdots \int_{-\sqrt{1-x_1^2-x_2^2-\cdots-x_{m-1}^2}}^{\sqrt{1-x_1^2-x_2^2-\cdots-x_{m-1}^2}} f(x_1,\ldots,x_m) \frac{\Gamma\left(\frac{n}{2}\right)}{\pi^{\frac{m}{2}} f(x_1,\ldots,x_m)\Gamma\left(\frac{n-m}{2}\right)} \left(1-\sum_{i=1}^{m} x_i^2\right)^{\frac{n-m-2}{2}} dx_1 dx_2 \cdots dx_m. \quad (B9)$$

By spherical symmetry, it is sufficient to compute the variance on x_1, but this trivially reduces to the result already obtained, since to compute it we may integrate out all the remaining coordinates $x_2,\ldots,x_m$. Therefore we find exactly

$$\langle x_i \rangle = 0$$

$$\langle x_i x_j \rangle = \delta_{ij}(\Delta x_i)^2 = \frac{\delta_{ij}}{n}. \quad (B10)$$

From similar reasoning, for sufficiently large n the distribution becomes Gaussian.

Therefore, the probability distribution over this reduced m sphere reduces to

$$P(x_1, x_2,\cdots,x_m) = \frac{\Gamma\left(\frac{n}{2}\right)}{\pi^{\frac{m}{2}}\Gamma\left(\frac{n-m}{2}\right)} \left(1-\sum_{i=1}^{m} x_i^2\right)^{\frac{n-m-2}{2}}, \quad (B11)$$

with suitable limits on the x_i. This is for the projection of an $(n-1)$ sphere to an m-dimensional subspace.

The limit of this distribution for $n - m \rightarrow \infty$ and sufficiently small x_i, $i \in \{1,\ldots,m\}$, may be approximated by a Gaussian with mean zero and a variance in every direction of $1/n$. This result agrees with previous work (Knaeble 2015), except on the condition needed, i.e., $n - m$ is large as opposed to merely n being large. The difference in this requirement means that as $m \rightarrow n$, where we project out fewer and fewer coordinates and finally none, the Gaussian approximation is found to fail wholly.

Appendix C
Projection of a Rotated Hypercube to Two Dimensions

Our analysis, both analytic and numeric, has largely been based on the projection of high-dimensional hyperballs. Here we consider the numerical projection of a randomly rotated high-dimensional hypercube to two dimensions. Although computing the X-ray of such a hypercube is straightforward, computing the projection of the boundary very quickly becomes computationally inaccessible. In particular, one needs to take the 2^n corners of the hypercube and project them to the lower dimension of interest and then compute the convex hull of those projected corners. This convex hull represents the "shadow" of the rotated hypercube under ordinary light (which is assumed to be unable to penetrate the object itself). In Figure 4 we illustrate this computation, comparing both the X-rays and shadows projected onto two dimensions of (a) a 33-dimensional hyperball and (b) a randomly rotated 20-dimensional hypercube (the highest dimension we could compute in a reasonable amount of time).

As can be seen, in sufficiently high dimensions the shadow of the randomly rotated hypercube, Figure 4(b), looks remarkably like that of the hyperball, Figure 4(a). Further, up to defining a suitable "diameter" to make a more rigorous comparison, the X-ray
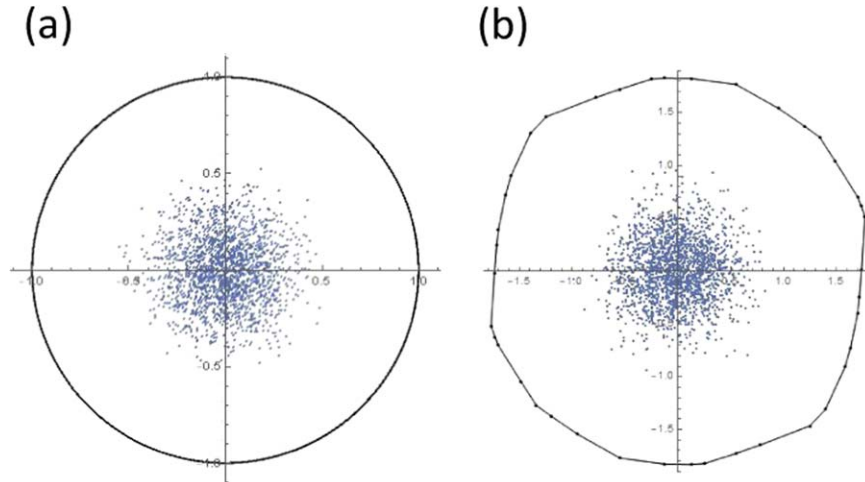

Figure 4. Plots of both the X-ray (as a scatter plot of 2000 points) where a higher density of points represents a larger weight of material being X-rayed and the "shadow" outline projection onto two dimensions of a (a) 33-dimensional hyperball and a (b) randomly oriented 20-dimensional hypercube. For the shadow of the hypercube, the dots along the outline represent the location of the corners there.

projection of such hypercubes appears remarkably similar to that of the hyperball (again, see Figure 4). Consequently, in our main manuscript we used a hyperball to compute the threshold illustrated by Figure 3 in even higher dimensions than we can manage for hypercubes.

Were much larger computational facilities available a more careful comparison should be possible, though even only a 42-dimensional hypercube entails over four trillion corners, so computing the projected boundary into any dimension greater than one (Knaeble 2015) would require major computational effort.

ORCID iDs

Zhi-Wei Wang ⓘ https://orcid.org/0000-0003-0847-1029

References

Adams, F. C. 2019, PhR, 807, 1
Carter, B. 1974, in IAU Symp. 63, Confrontation of Cosmological Theories (Cambridge: Cambridge Univ. Press), 291
Ćirković, M. M. 2016, AsBio, 16, 737
Deutsch, D. 2011, The Beginning of Infinity: Explanations That Transform The World (London: Penguin), 96
Diaconis, P., & Freedman, D. 1984, AnSta, 12, 793
Dicke, R. H. 1961, Natur, 192, 440
Eddington, A. S. 1936, Relativity Theory of Protons and Electrons (Cambridge: Cambridge Univ. Press)
Eddington, A. S. 1939, The Philosophy of Physical Science (Tarner Lectures 1938) (Cambridge: Cambridge Univ. Press)
Hoyle, F. 1954, ApJS, 1, 121
Klartag, B. 2007, InMat, 168, 91
Knaeble, B. 2015, Gen. Math. Notes, 26, 119
Martel, H., Shapiro, P. R., & Weinberg, S. 1998, ApJ, 492, 29
Milman, V. D. 1988, Astérisque, 157, 273
Overbye, D. 2020, The Search for E.T. Goes on Hold, for Now, New York Times, 2020 March 23
Piran, T., Jimenez, R., Cuesta, A. J., Simpson, F., & Verde, L. 2016, PhRvL, 116, 081301
Siegel, E. 2018, How Many Fundamental Constants Does It Take To Explain The Universe?, Forbes, 2018 November 16
Thorne, K. S., Wheeler, J. A., & Misner, C. W. 2000, Gravitation (San Francisco, CA: Freeman)
Wang, Z. W., & Braunstein, S. L. 2023, NatAs, 7, 755
Weinberg, S. 1987, PhRvL, 59, 2607
Wilde, O. 1889, The Decay of Lying: A Dialogue, The Nineteenth Century and After: A Monthly Review, ed. J. Knowles, 25, 35